Ensemble and Single-Molecule Fluorescence Spectroscopy of a Calcium-Ion Indicator Dye

Sangram Bagh and Matthew F. Paige*

Department of Chemistry, University Of Saskatchewan, 110 Science Place, Saskatoon, SK, S7N5C9, Canada

Received: February 2, 2006; In Final Form: April 3, 2006

The spectroscopic properties of Calcium Green 2 (CG-2), a dual-fluorophore Ca^{2+} indicator dye, were characterized by a combination of steady state and time-resolved ensemble spectroscopic measurements, molecular mechanics calculations and single-molecule fluorescence spectroscopy. It was found that in Ca^{2+} free solutions, CG-2 exists primarily as a highly quenched intramolecular dimer, but when bound to Ca^{2+}, the molecule adopts an extended, fluorescent conformation. The difference in emission properties of these two CG-2 conformations is explained in terms of simple exciton theory. Through single-molecule fluorescence measurements, we have shown that the bulk increase in ensemble fluorescence intensity correlates with a simple statistical increase in the number of fluorescent molecules in solution. In addition, we have also observed that the majority of CG-2 molecules photobleach in a single step, despite the molecule possessing two distinct fluorophores. A small fraction of molecules photobleach in multiple steps or show a series of transitions between emissive and nonemissive fluorescent states ("blinking"). We rationalize these photophysical phenomena using a simple model based on dipole−dipole Förster coupling between fluorophores in conjunction with irreversible photodamage to one of the constituent chromophores.

1. Introduction

The ability to detect and quantify intracellular free Ca^{2+} is of singular importance in understanding a diverse range of cellular processes, particularly those involving intracellular messaging.[1−4] Of special importance in this regard has been the development of fluorescent Ca^{2+} indicator dyes for in vivo biological studies involving measurement of cytosolic free Ca^{2+} levels. In general, Ca^{2+} indicators are molecules that, in the absence of Ca^{2+} are essentially nonfluorescent but upon exposure to Ca^{2+} yield a product with strong fluorescence emission. There are currently a wide variety of Ca^{2+} indicators available, ranging from simple, small organic molecules[5−8] to protein constructs based on autofluorescent protein fluorescence resonance energy transfer pairs ("cameleons").[9−12]

In terms of organic indicator dye molecules, a subset of compounds that have proven to be particularly well-suited for cytosolic Ca^{2+} measurements are those based on 1,2 bis(o-aminophenoxy)ethane-*N*,*N*,*N*′*N*′-tetracetic acid (dubbed "BAPTA").[5−7,13] BAPTA is a variant of the well-known chelating agent, ethylene glycol bis(*β*-aminoethyl ether)-*N*,*N*,*N*′,*N*′-tetracetic acid (EGTA), in which constituent methylene groups have been substituted with benzene groups. Chemical structures for EGTA and BAPTA are shown in Figure 1A,B. BAPTA-based indicator dyes have excellent Ca^{2+} binding properties, including low dissociation constants, rapid binding kinetics and high binding selectivity, making them particularly well suited for use in vivo.

Basic spectroscopic characterization of the BAPTA moiety itself has been carried out by Tsien.[6] It was found that binding of Ca^{2+} by BAPTA gave rise to a significant blue shift in its UV absorption spectrum. The spectrum of the molecule in the unbound state resembled that of a simple dialkylaniline, but upon Ca^{2+} binding, the spectrum resembled an alkylbenzene. As such,

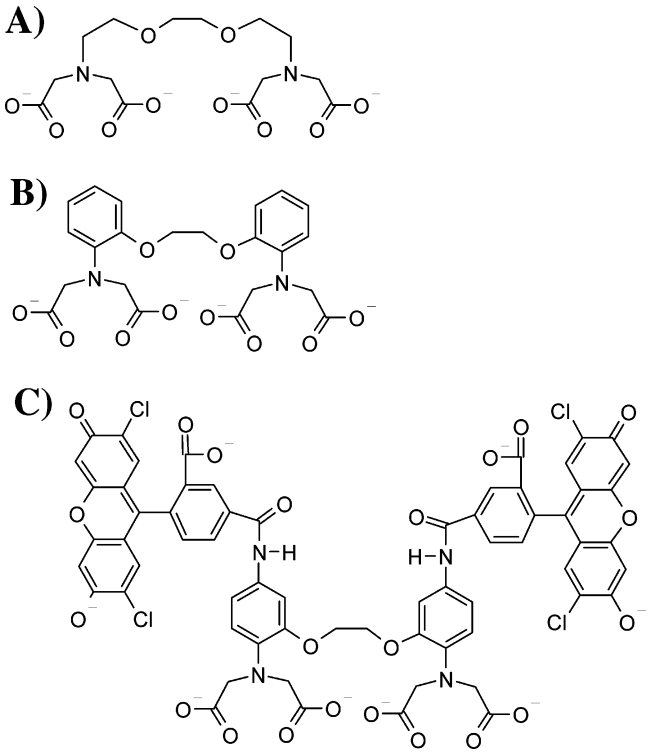

Figure 1. Chemical structures of (A) EGTA, (B) BAPTA, and (C) Calcium Green 2.

it was proposed that the observed spectral changes are caused by the breaking of conjugation between the aromatic ring structures and the nonbonding electrons on the amine groups when the nitrogen ring-bonds twist during Ca^{2+} chelation. Though informative, such shifts in UV absorption bands are not well suited for optical detection in cellular environments, and considerable effort has been made to incorporate fluorophores that absorb and emit in the visible region into BAPTA-

* Corresponding author. E-mail: matthew.paige@sask.usask.ca. Tel: 1-306-966-4665. Fax: 1-306-966-4730.

10.1021/jp060719e CCC: $33.50
Published on Web 05/12/2006

based indicator dyes. Arguably the most successful approach in this regard has been to attach a strongly fluorescent functional group directly to the constituent benzene ring, usually ortho to the amine group. Of particular note are the indicator dyes "rhod-1" and "fluo-1", in which variants of rhodamine and fluorescein fluorophores have been linked to BAPTA to yield indicators that emit strongly in the visible region.[13] Since their original chemical synthesis, these molecules have been the basis for many closely related commercial variants that have a range of absorption and emission properties. Despite the widespread application of these indicators, many aspects of their spectroscopic behavior remains poorly understood and need to be thoroughly explored.

Of particular interest to our research group is the commercial indicator known as Calcium Green 2 (CG-2; Molecular Probes/Invitrogen). CG-2 is very well suited for in vivo Ca^{2+} detection; the manufacturer reports an almost 100-fold increase in fluorescence intensity on Ca^{2+} chelation, a low dissociation constant ($K_d = 0.55\ \mu M$), and an absorption maximum ($\epsilon_{max} \sim 503$ nm) that is reasonably well-matched to excitation by conventional laser sources.[14] The chemical structure of this indicator is shown in Figure 1C. CG-2 is different from many commercial indicators in that it is a difluorophoric system. Instead, of a single rhodamine or fluorescein unit attached to the benzene group, two identical fluorophores have been added to produce a symmetrical molecule. The mechanism that gives rise to an increase in fluorescence intensity with Ca^{2+} binding is not immediately apparent from inspection of CG-2's chemical structure. The manufacturer suggests that intramolecular "self-quenching" of fluorophores in the absence of Ca^{2+} might be taking place, though there is no published evidence to support or refute this. In our view, it seems feasible for this system to assume a conformation that promotes nonfluorescent exciton (intramolecular H-dimer) formation, possibly by adopting a coplanar arrangement of the two fluorophores.[15]

Although the primary goal of these studies is to elucidate the mechanism of action of CG-2 via conventional spectroscopic methods, we also wish to explore the suitability of this indicator dye for the study, in a simple and controlled way, of excitonic behavior in a simple dimer system at the single-molecule level. In addition to being a generally useful spectroscopic method of analysis, single-molecule (SM) fluorescence spectroscopy has proven to be a powerful tool for probing excitonic coupling in a range of multichromophoric systems, ranging from light-harvesting complexes, to donor−acceptor substituted biopolymers, to multifluorophoric dendrimers and proteins.[16−20] SM fluorescence measurements have shown that there exists a surprising number of common features in coupled systems, of particular note being the tendency of multifluorophoric molecules to show a collective quenching of fluorescence emission.[17,20−22] This has tentatively been linked to the formation of photoinduced trap states, though much work still remains to be done in this area.

Many of the SM investigations that have been carried out on coupled fluorophore systems to date have been very challenging to interpret, because the systems that have been studied typically contain large numbers of fluorophores. Hernando et al.[23] attempted to address this issue by studying exciton formation in a simple test system consisting of a tetramethylrhodamine-5-isothiocyante (TRITC) dimer, and comparing the results with monomeric TRITC alone. It was found that in this system, only weakly coupled TRITC dimers were fluorescent, and that having one unit in a dark (likely triplet) state can lead to emission quenching in the other subunit. Though providing good insight into the nature of the exciton formation and collective emission quenching via photoinduced trap states, one shortcoming of the system used in this study was that the dimers were thought to exist in a number of different conformations, ranging from a compact arrangement in which the chromophore units are held in close proximity, to an extended conformation in which the chromophores are far apart. We believe that, should the exciton model prove valid for describing the behavior of CG-2, its Ca^{2+} bound form should be structurally rigid and kinetically stable, making it ideally suited for SM investigation of fluorophore coupling in dimeric systems.

2. Experimental Section

(A) Sample Preparation for Ensemble Measurements. CG-2 (octapotassium salt) and calcium buffers that contain well-defined concentrations of "free" Ca^{2+} (not chelated, herein referred to as $Ca^{2+}{}_{free}$) were purchased from Invitrogen (Invitrogen Canada Inc., Burlington, ON., Canada) and used as received. The preparation, calculation of $[Ca^{2+}]_{free}$ and the underlying chemistry for the Ca^{2+} buffers used here have been described in detail by Tsien.[7] Briefly, the buffers are based on the Ca^{2+} chelating agent, EGTA, and make use of the propensity of EGTA to bind with Ca^{2+} to regulate the amount of $Ca^{2+}{}_{free}$ available in solution. For ensemble measurements, an initial stock solution of CG-2 was prepared by dissolving the bulk solid in pH 7.2 TRIS buffer to give a final stock solution concentration of approximately 0.3 mM. Stock solutions of CG-2 were kept refrigerated in the dark until needed. Immediately before taking spectroscopic measurements, aliquots of the stock solution were added to the different $Ca^{2+}{}_{free}$ buffers, giving final concentrations of CG-2 of around 1.5 μM for absorbance measurements and around 0.2 μM for emission measurements. We note that the solutions made from mixing the CG-2 stock solution and the Ca^{2+} buffers became less fluorescent after several days of storage, suggesting a slow decomposition of the fluorescent product. Care was taken to use only freshly prepared samples for spectroscopic measurements.

(B) Ensemble Spectroscopy Measurements. Absorption spectra were collected with a Varian Cary 500 UV−vis spectrometer and steady-state emission spectra were collected using a SPEX 212 spectrofluorometer. Measurements were carried out in either 1.0 cm × 1.0 cm disposable polystyrene cuvettes (absorption) or quartz cuvettes (emission), at room temperature. Fluorescence lifetimes were measured using the method of time-correlated single-photon counting (TCSPC). Briefly, the output from a mode-locked, frequency-doubled femtosecond Ti-sapphire laser was directed onto the sample solutions contained in 1.0 cm × 1.0 cm quartz cuvettes. The decay rate of fluorescence was determined by TCSPC, with emission collected at the magic angle. Excitation was performed at 490 nm, with an emission collection wavelength of 536 nm. Decay profiles were fit using a nonlinear least squares reconvolution procedure based on the Marquardt algorithm. The quality of fit was assessed through the value of the reduced χ^2 and through the distribution of weighted residuals.

(C) Single Molecule Microscope Setup and Sample Preparation. Single-molecule fluorescence measurements were carried out using a wide-field epifluorescence microscope (Nikon TE2000, Nikon, Canada), with 488 nm continuous-wave excitation. The linearly polarized output from an argon-ion laser (Melles Griot, Carlsbad, CA, U.S.A.) was directed through a series of neutral-density filters to adjust laser power, a quarter-waveplate to generate circularly polarized light and was then

focused onto the back focal-plane of a 60×, 1.4 NA oil-immersion microscope objective with a 500 mm focusing lens. Excitation light was reflected onto the sample using a dichroic 500DRLP beam splitter (Omega Optical, Brattleboro, VT, U.S.A.). Fluorescence emission from the sample was passed through two long-pass filters (500AELP) to attenuate residual excitation light and directed onto a front-illuminated CCD photodetector (Cascade 512F, Photometrics, Tucson, AZ, U.S.A.). Data analysis was carried out using the software MetaMorph (Universal Imaging, Downington, PA, U.S.A.). Excitation intensities reported in the body of the text were determined by measuring the excitation power at the focal plane and dividing by the experimentally measured illumination area.

Samples for SM fluorescence experiments were prepared by first spin-casting dilute solutions ($\sim 10^{-9}-10^{-10}$ M) of CG-2 in appropriate Ca^{2+} buffers onto clean microscope coverglass slides, then spin-casting a layer of dilute polymer (2 wt % poly(vinyl alcohol) in Millipore water) onto the coverglass. Careful control samples consisting of the coverglass alone and coverglass treated with the different buffers, solvents and polymers in the absence of CG-2 were imaged to ensure observed signals were from CG-2 alone. In all cases, the control samples showed no fluorescent impurities when imaged at the single-molecule level.

3. Results and Discussion

(A) Bulk Spectroscopic Measurements. A series of absorption spectra were collected in which the concentration of CG-2 was kept fixed but $[Ca^{2+}]_{free}$ was systematically varied (representative spectra shown in Figure 2A−E). Each absorption spectrum consisted of two strongly overlapping peaks, with the two peak maxima located at 490 and 508 nm. As $[Ca^{2+}]_{free}$ was increased, the intensity of the longer wavelength peak increased relative to that of the shorter wavelength peak. The appearance of two peaks in the absorption spectrum is consistent with the coexistence of two different types of rhodamine species in solution. There are two likely mechanisms that can result in the formation of multiple species in solution, both of which may be acting simultaneously for this system. The first possible source is that the rhodamine groups of different CG-2 molecules might associate with one another, giving rise to equilibrium between intermolecular CG-2 dimers and their component monomers (intermolecular dimerization). The second, and in our view the dominant mechanism in this system, is formation of two chemical species associated with a Ca^{2+} binding−dissociation reaction. In terms of the former, it is well-known that a number of xanthene (rhodamine-like), cyanine and acridine dyes have a strong tendency to dimerize in solution or when confined in structures such as liposomes (see, for example, refs 24−26). To assess the possibility that intermolecular dimerization might play an important role over the concentration range of interest, we measured absorption spectra for Ca^{2+} free buffers over a CG-2 concentration range of ca. 1−15 μM and found no detectable change in the relative intensities of the two absorbance peaks with CG-2 concentration. If intermolecular dimerization were occurring to a substantial degree, dilution would perturb the monomer−dimer equilibrium distribution and thus alter the relative absorption peak height ratios. In general, one expects intermolecular dimerization effects to become important at dye concentrations significantly higher (typically on the order of $\sim$ 10 mM[26]) than those used here. These measurements, in conjunction with the strong $[Ca^{2+}]_{free}$ dependence of the long wavelength peak, indicate that we can reasonably attribute the observed spectral changes to intramolecular changes in CG-2 associated with Ca^{2+} binding. In addition, the appearance of two peaks in the absorption spectra is also in excellent agreement with the results expected from Kasha's exciton model for parallel transition dipoles in molecular dimers,[15] as will be discussed in further detail later in this article.

Steady-state fluorescence emission spectra were also collected for CG-2 solutions over a range of different $[Ca^{2+}]_{free}$. A series of emission spectra showing fluorescence emission intensity as a function of $[Ca^{2+}]_{free}$ is shown in Figure 3. As expected, the fluorescence intensity increases markedly with increasing $[Ca^{2+}]_{free}$. The fluorescence intensity was found to reach a maximum at $[Ca^{2+}]_{free}$ of approximately 39 μM and increasing the concentration beyond this level had no further significant effect on the measured signal. This indicates that CG-2 was saturated with calcium at this concentration. On the basis of the total integrated peak areas, we found that the emission intensity of CG-2 at $[Ca^{2+}]_{free} = 39$ μM was 38 times greater than that of the $[Ca^{2+}]_{free} = 0$ μM sample. An equilibrium dissociation constant (K_d) and Ca^{2+} binding stoichiometry for the CG-2/Ca^{2+} complex can be determined from the emission data by making use of a simple equilibrium binding model that assumes proportionality of fluorescence emission intensity with concentration of Ca^{2+}-bound CG-2.[7] Defining the following dissociation equilibrium and corresponding dissociation constant:

$$\text{CG-2}\cdot\text{Ca}^{2+}{}_{(n)} = \text{CG-2} + n\text{Ca}^{2+} \tag{1}$$

$$K_d = \frac{[\text{CG-2}][\text{Ca}^{2+}]^n}{[\text{CG-2}\cdot\text{Ca}^{2+}{}_{(n)}]} \tag{2}$$

where CG-2·$Ca^{2+}{}_{(n)}$ is the CG-2/Ca^{2+} complex. Assuming that the experimentally measured emission intensity is proportional to the reagent concentration, we can derive the following expression:

$$\log\left(\frac{F_x - F_{min}}{F_{max} - F_x}\right) = n \log [\text{Ca}^{2+}] - \log K_d \tag{3}$$

where F_x, F_{min} and F_{max} are the fluorescent intensities corresponding to the $[Ca^{2+}]_{free}$ of interest, the intensity at $[Ca^{2+}]_{free} = 0$ and the intensity measured at the maximum value of $[Ca^{2+}]_{free}$. A plot of the variable on the left-hand side of eq 3 versus log$[Ca^{2+}]$ is shown in Figure 3B. From the x-intercept, we calculate $K_d = 1.13$ μM, and a slope of 1.10, the latter indicating one-to-one binding stoichiometry between CG-2 and Ca^{2+}. In our hands, the measured K_d was approximately twice as large as the value reported by the manufacturer.[14] Similar measurements taken using a set of higher (albeit less accurately known) $[Ca^{2+}]_{free}$ buffers yielded comparably large K_d values. The reason for the discrepancy between the manufacturer's value and our values is not currently clear.

The increase in fluorescence emission intensity correlates with the increase in intensity of the high wavelength absorbance peak. This indicates that CG-2 exists in either one of two states: the first, a strongly fluorescent molecule with an absorption maxima in the high wavelength region of the spectrum when bound to Ca^{2+}, and the second, a blue-shifted, nonfluorescent molecule in the absence of Ca^{2+}. The latter two properties, a blue-shifted (relative to the monomer) absorption spectrum accompanied by fluorescence quenching, are well-known characteristics of exciton formation between planar molecules. In his work on the subject of excitons, Kasha presented a classical vector model describing exciton formation in dimeric systems.[15] Dimer

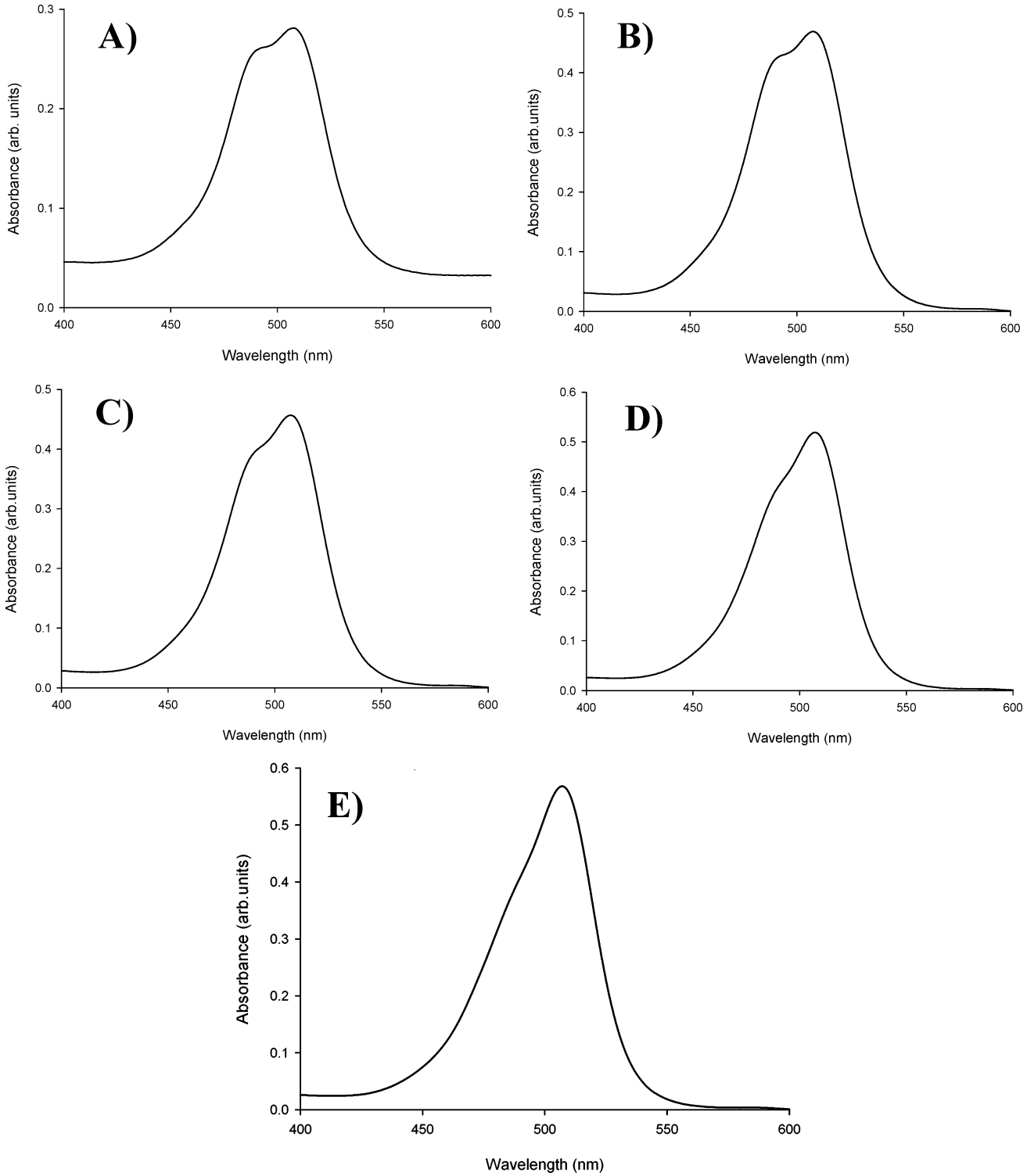

Figure 2. Series of absorbance spectra showing the effect of $[Ca^{2+}]_{free}$ on spectral peak shape. For all spectra, the CG-2 concentration was kept constant at 1.5 μM. The $[Ca^{2+}]_{free}$ for each spectrum is (A) 0.00 μM, (B) 0.04 μM, (C) 0.23 μM, (D) 0.60 μM, and (E) 1.35 μm.

association in which the transition dipole moments for the component molecules form an oblique angle to one another (Figure 4) was predicted to lead to a splitting of the monomer energy levels into a red- and blue-shifted level, with a splitting energy given by

$$\Delta\epsilon = \frac{1}{4\pi\epsilon_0}\frac{2|M|^2}{r_{uv}{}^3}(\cos\alpha - 3\cos\theta_1\cos\theta_2) \qquad (4)$$

where M is the monomer transition dipole moment, r_{uv} is the center-to-center distance between the two transition dipole moments, α is the angle between the molecular planes of the two fluorophores and $\theta_{1,2}$ are the angles between the molecular centers and the transition dipole moment of the two fluorophores. For the case of parallel transition dipoles ($\alpha = 0$), the transition from the ground state to the lower (red-shifted, transition dipoles out of phase) energy state is forbidden. Additionally for parallel transition dipoles, there is often a rapid conversion from the upper to the lower exciton state, from which radiative transitions are forbidden. This generally results in

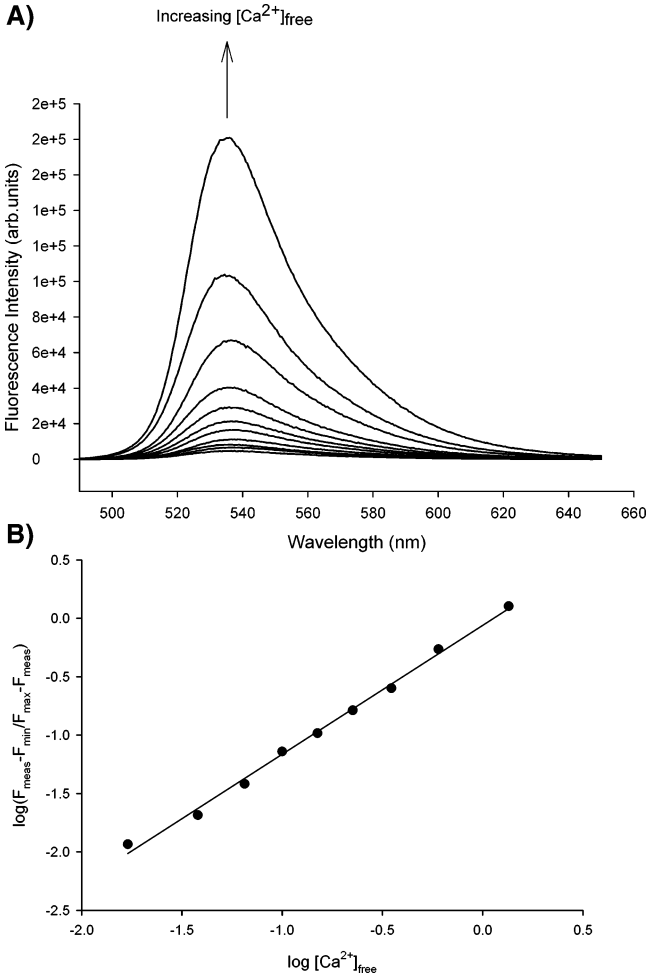

Figure 3. (A) Series of fluorescence emission spectra showing the change in emission intensity as a function of $[Ca^{2+}]_{free}$ ($[Ca^{2+}]_{free}$ ranges from 0 to 39 μM, [CG-2] = 0.20 μM). (B) Plot used to determine K_d and Ca^{2+}/CG-2 binding stoichiometry.

radiationless intersystem crossing to a triplet state and the coupled system does not fluoresce.

Exciton splitting in dimeric systems typically leads to a blue shift in the monomer absorption spectrum in the range 1000−2500 cm^{-1}. If we assume that, for CG-2 in the presence of Ca^{2+}, each constituent rhodamine unit behaves as an independent monomer, then we can attribute the high-wavelength peak in the absorption spectra from Figure 2 as being that of the pure monomer. The absorption peak that is blue-shifted from this by 18 nm falls well within the range expected from Kasha's vector model.

In an attempt to better understand the nature of the structure of CG-2 in the Ca^{2+} bound and unbound states, we have carried out some simple structure optimization and conformational search calculations using molecular mechanics (MMFF, Spartan '04). It should be noted that these calculations are carried out for molecules in a vacuum and that the true solution structures might differ from those calculated using this approach. With this caveat, we view these calculations as a useful, "semiquantitative" approach to understand the effect of Ca^{2+} binding on molecular conformations.

For the conformational search calculations, we chose for the initial structure of the unbound state of CG-2 the energy minimized structure of the molecule, and for the Ca^{2+}-bound state, we modeled the Ca^{2+} binding site as a calcium ion coordinated with the six binding moieties of BAPTA. This initial

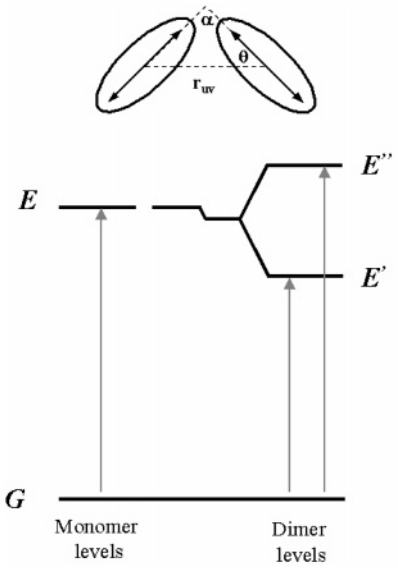

Figure 4. Schematic model of excitonic splitting in the CG-2 system. The illustration at the top of the figure illustrates the simple vector model used to describe the interaction between transition dipole moments (represented by the double arrows) of the two constituent fluorophores (oval represents long axis of the molecule). The variables α, θ and r_{uv} are described in eq 4.

structure was based on the structure of CaEGTA complexes as determined by X-ray crystallography studies.[27,28]

The lowest energy conformers we found had structures such as those shown in Figure 5A−C. As shown in Figure 5A,B the unbound state of CG-2 tends to adopt a conformation in which the two rhodamine rings are approximately coplanar. From these structures, we estimate the distance between the centers of the two rhodamine groups as approximately 0.7 nm, the angle $\alpha \sim 0°$ and $\theta \sim 65°$. Again, this is exactly the type of structure that is anticipated to lead to formation of exciton states. Substituting typical values measured for this preferred conformer into eq 4, and calculating the transition dipole moment from the appropriate absorption spectrum of CG-2 (calculated using the software PHOTOCHEMCAD written by Lindsey et al.[29]), we calculate a spectral blue shift of around 16 nm, which is in excellent agreement with the experimental value of 18 nm. This agreement between experimental and calculated values also provides reassurance that differences between the optimized vacuum structures and those in solution are of minimal importance. Although the conformers shown here were significantly preferred over other noncoplanar geometries, it seems plausible that some small fraction of molecules might be found in conformations where exciton formation does not take place. In addition to the presence of trace amounts of $Ca^{2+}{}_{free}$ in the nominal "zero" Ca^{2+} concentration buffer, this may be a source of the small residual fluorescence we observe in the emission spectrum.

Of additional interest is the Ca^{2+}-bound form of CG-2. The preferred conformer model indicates that, upon Ca^{2+} binding, the two rhodamine units move apart both in distance (center-to-center distance of the rhodamine units approximately doubles to 1.2 nm) and in relative orientation (angle between molecular planes $\sim 55°$) as compared to CG-2 without Ca^{2+}. According to eq 4, these two conformational changes should have a drastic cumulative affect on the efficiency of exciton formation; we calculate that the energy splitting for the Ca^{2+}-bound form should be <5% of that found for the Ca^{2+}-free form. This correlates with the appearance of the high-wavelength absorption peak and the onset of fluorescence. We believe that the

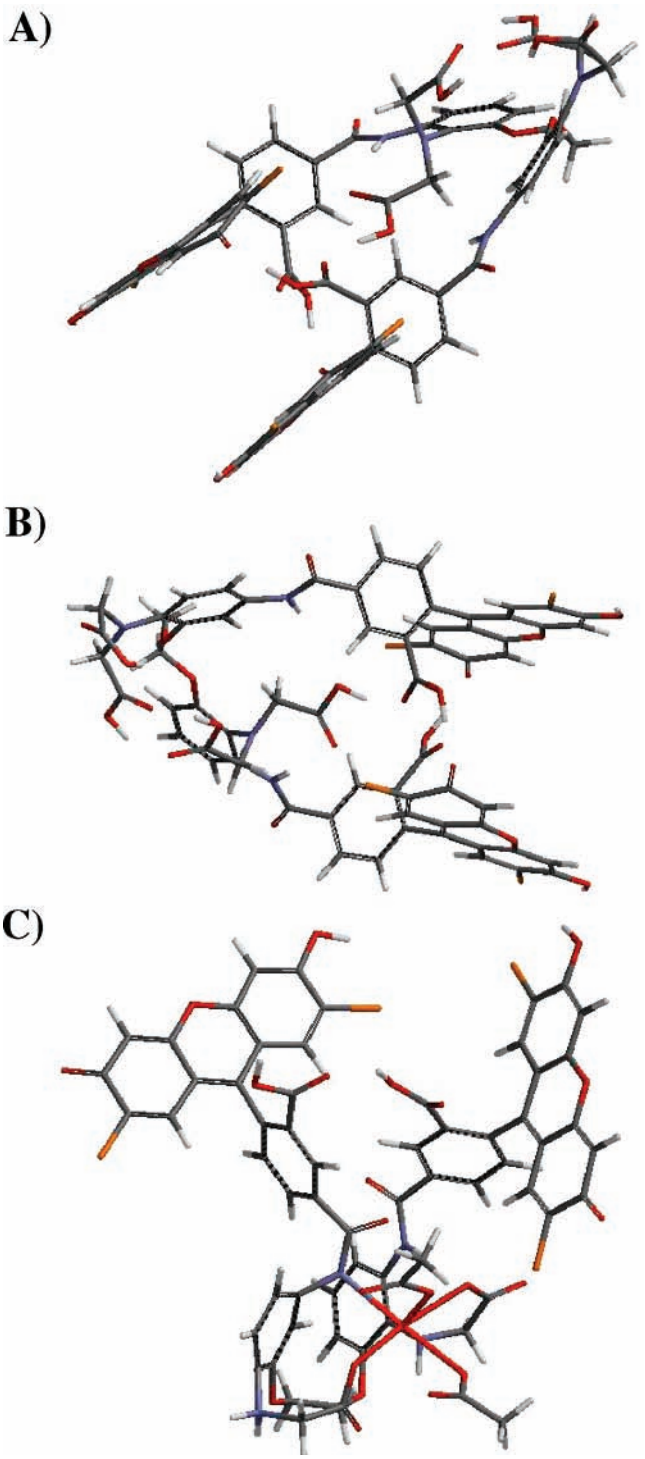

Figure 5. CG-2 structural conformers calculated using molecular mechanics (MMFF) conformational search. (A) and (B) are the structures calculated in the absence of Ca^{2+} (two different views), and (C) is the structure that is predicted after CG-2 binding of Ca^{2+}.

conformational change that occurs with binding of Ca^{2+} is such that the ability of the system to form an exciton is negligible and that the rhodamine subunits will essentially behave as independent monomers. This suggests that in terms of a mechanism of action for CG-2, as more Ca^{2+} is added to solution, the relative proportions of the quenched exciton form of CG-2 and the emissive form shifts, resulting in stronger net fluorescence emission.

To gain further insight into the mechanism of operation of this system, fluorescence lifetimes of CG-2 were measured over

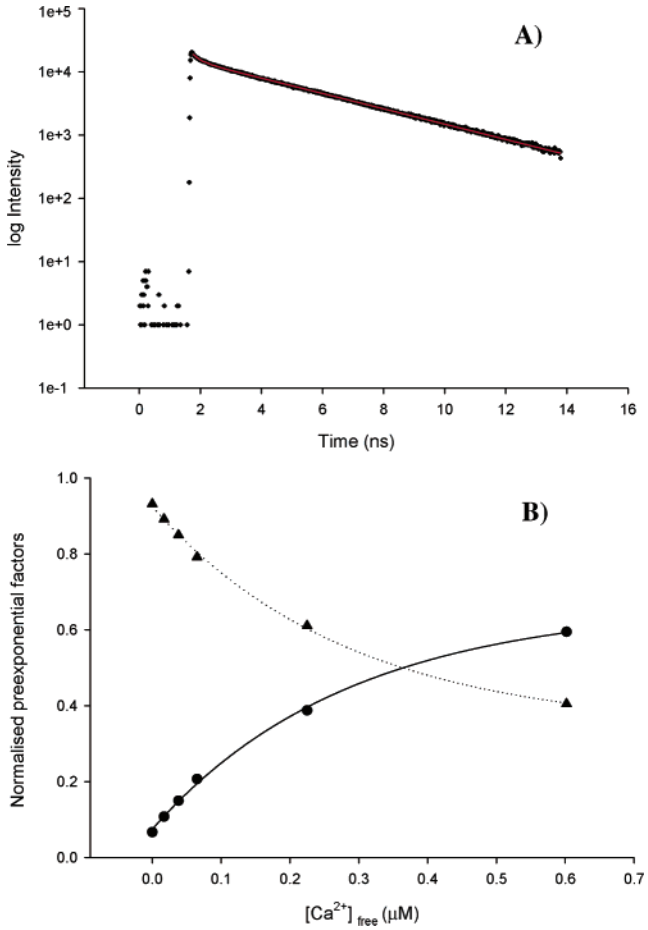

Figure 6. (A) Typical fluorescence lifetime measurement taken from a 1.5 μM solution of CG-2 in 0.602 μM $[Ca^{2+}]_{free}$. The solid line is a double-exponential fit obtained using the fitting procedure described in the main text. (B) Plot showing dependence of fluorescence lifetime preexponential factors on $[Ca^{2+}]_{free}$. The filled circles correspond to the slow (3.5 ns) lifetime component whereas the solid triangles correspond to the fast (0.3 ns) lifetime component.

a range of $[Ca^{2+}]_{free}$ via TCSPC. Results from a typical measurement taken at a $[Ca^{2+}]_{free}$ of 0.602 μM are shown in Figure 6A, along with an appropriate decay fit. For the range of $[Ca^{2+}]_{free}$ explored, it was found that the fluorescence decay profiles were best fit by two adjustable exponential lifetimes and two adjustable preexponential factors according to the equation

$$I(t) = \sum_{i=1}^{n} \alpha_i e^{-t/\tau_i} \qquad (5)$$

where $I(t)$ is the time-dependent fluorescence intensity decay, α_i are the preexponential factors and τ_i are the fluorescence lifetimes. The measurements gave a long lifetime component equal to 3.5 $\pm$ 0.1 ns, and a short component equal to 0.3 $\pm$ 0.1 ns. It was also found that though the magnitude of the preexponential factor depended strongly on the $[Ca^{2+}]_{free}$, the same fluorescence lifetimes were obtained over the entire range of $[Ca^{2+}]_{free}$ measured. As $[Ca^{2+}]_{free}$ was increased, the magnitude of the long lifetime component increased and the magnitude of the short lifetime component correspondingly decreased. The magnitude of the preexponential factors is plotted as a function of $[Ca^{2+}]_{free}$ in Figure 6B. If one assumes that the ratio of preexponential factors for the two lifetimes represents the ratio of concentrations of the relevant species, one can fit

the data from Figure 6B to the same simple equilibrium binding model described by eq 3. Doing so yields a dissociation constant equal to $K_d = 0.52\ \mu$M, which is in good agreement with the value provided by the manufacturer, though slightly different from the values we measured previously using steady-state emission. As was the case with the steady-state spectroscopic measurements, these results are consistent with the coexistence of two distinct chemical species whose relative amounts depend on the concentration of free Ca^{2+}.

We note that the values measured for lifetimes and the presence of two distinct, $[Ca^{2+}]_{free}$ dependent components in the lifetime decay are very similar to the results obtained by Sanders et al.[30] ($\alpha_1 = 0.97$, $\tau_1 = 0.46$ ns and $\alpha_2 = 0.03$, $\tau_2 = 3.53$ ns at nominal zero $[Ca^{2+}]_{free}$) in their fluorescence lifetime imaging experiments in rat myocyte cells using Calcium Green-1 (CG-1) as a nonspecific stain. CG-1, another member of the BAPTA-based indicator dye family, contains a single fluorophore that is identical to the constituent fluorophores in CG-2, and as such it is not surprising that we get comparable lifetimes. Sanders attributed the existence of two lifetimes to the dual existence of the free and Ca^{2+} bound indicator dyes, and the change in magnitude of amplitudes follows the relative change in concentration of the $Ca^{2+}{}_{free}$. In the case of CG-2, we also attribute the observed trend to the formation of the CG-2/Ca^{2+} complex. The increase in magnitude of the long lifetime component simply follows the increase in quantity of the strongly fluorescent complex, and similarly, the decrease in magnitude of the short component follows the decrease in quantity of the quenched Ca^{2+} free intramolecular dimer.

In summary, the combination of absorption, steady-state and time-resolved fluorescence measurements, in conjunction with structure optimization calculations indicates that the mechanism of Ca^{2+} sensitivity in this indicator dye is the formation and subsequent destruction of the intramolecular exciton on binding of Ca^{2+}.

(B) Single Molecule Fluorescence Measurements. Samples prepared for single-molecule imaging experiments revealed a series of discrete fluorescent spots on a dark background when imaged in the microscope. A typical fluorescence image of a sample prepared in this way at a $[Ca^{2+}]_{free}$ of 10 μM is shown in Figure 7A. The spots were ~300 nm in diameter (determined by calibrating the detector pixel size against a standard USAF test target), which is consistent with the diffraction-limited size expected for an individual molecule. Upon continuous laser illumination at an excitation intensity of 0.9 kW/cm^2, the majority of the fluorescent spots photobleached in a single, discrete step, which we take as the signature of an individual molecule. Several hundred individual molecules of CG-2 were observed, and of these molecules, approximately 94% photobleached in a single step (typical time-trace shown in Figure 7B-i) with the remaining fraction showing more complex photobleaching behavior (Figure 7B-ii,iii discussed in more detail later). We note that after extended continuous illumination (minutes), molecules of CG-2 that photobleached in a single step did not return to an emissive state (irreversible photobleaching). The signal intensities we observed for individual CG-2 molecules were comparable with the signals we have measured under similar imaging conditions for single rhodamine 6G molecules.[31] It should be noted that the excitation intensities used here are well below the optical saturation intensity of the fluorophore (for example, Schmidt et al.[32] measured a typical saturation intensity for tetramethylrhodamine as ~6 kW/cm^2).

It is interesting to consider the mechanism of fluorescence intensity increase for CG-2 solutions from the point of view of single-molecule experiments. One can conceive of two possible routes by which the overall solution fluorescence emission in a

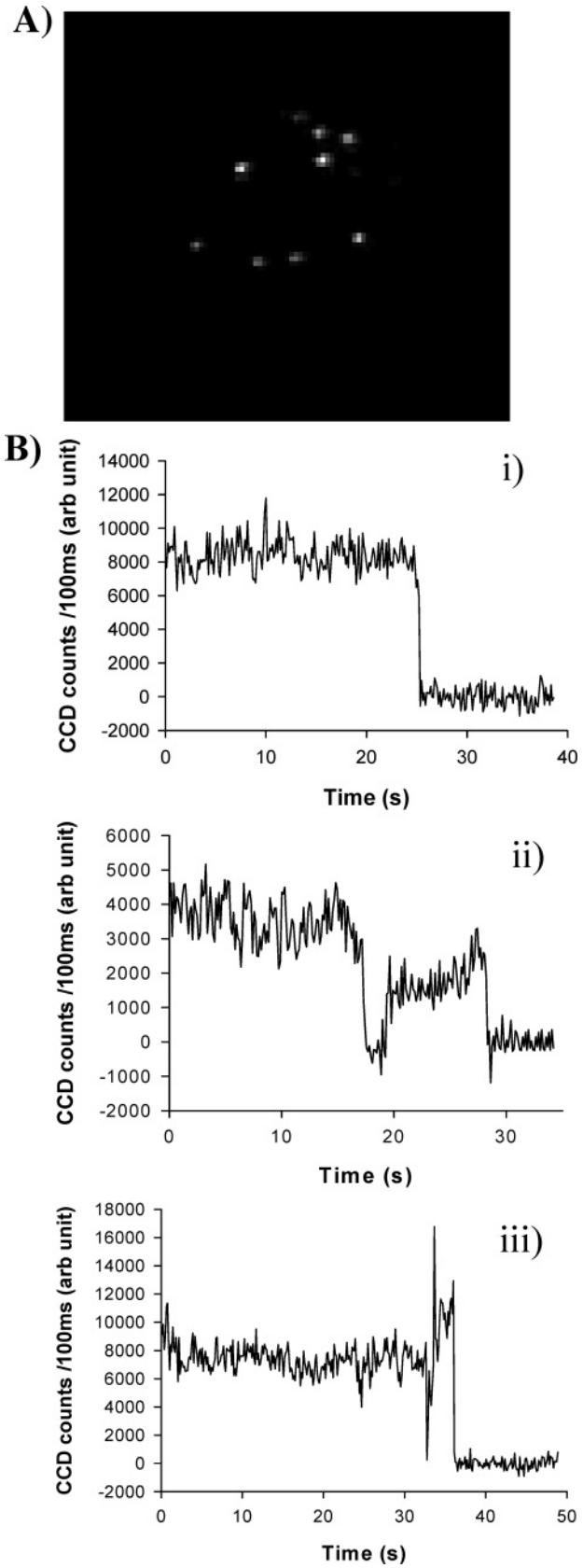

Figure 7. (A) Single-molecule fluorescence image of CG-2 (dye concentration ~ 10^{-9} M, $[Ca^{2+}]_{free}$ =10 μM, excitation intensity 0.9 kW/cm^2). The image size is approximately 10 μm × 13 μm. (B) Single-molecule time traces of CG-2 showing (i) single-step photobleaching and (ii) and (iii) complex blinking behavior.

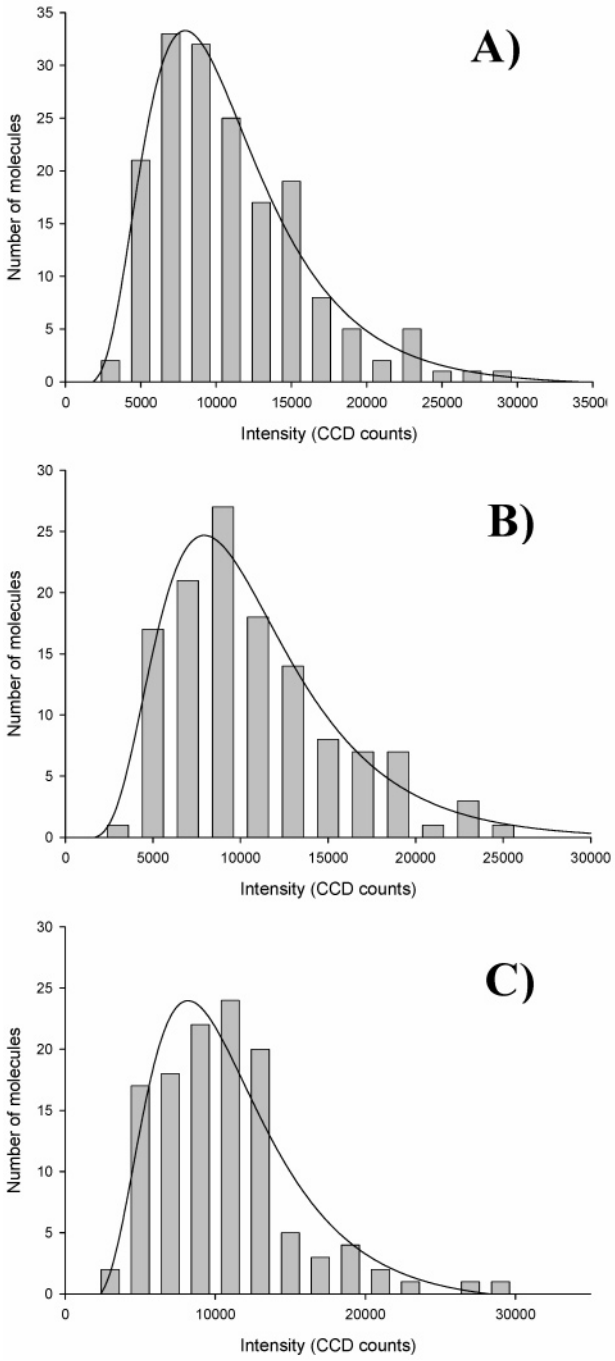

Figure 8. Histograms showing fluorescence intensity of individual CG-2 molecules as a function of $[Ca^{2+}]_{free}$, with a log-normal fit: (A) $[Ca^{2+}]_{free} = 0$ μM; (B) $[Ca^{2+}]_{free} = 10$ μM; (C) $[Ca^{2+}]_{free} = 100$ μM.

Ca^{2+} sensor dye system would increase; the first is that each individual molecule of CG-2 emits with increasingly greater intensity as more Ca^{2+} is added to solution, whereas the second, and that which is obviously supported by the ensemble spectroscopic measurements, is that there are simply two discrete forms of the dye (emissive and quenched) and increased emission comes from a statistical increase in the number of emissive molecules. One can differentiate between these two possibilities by using single-molecule measurements. Figure 8A−C shows histograms of single-molecule fluorescence intensities (measured in CCD counts at fixed integration time and multiplier gain) recorded at three different Ca^{2+} concentrations, ranging from below the Ca^{2+} saturation level to significantly above it. Histograms produced in this way showed a single, slightly skewed peak. The skewed Gaussian shape of the intensity histograms is attributed to the random orientation of molecules in the sample in conjunction with imperfectly circularly polarized light (a similarly shaped histogram was produced from a control sample consisting of individual rhodamine 6G molecules measured under the same imaging conditions). The histograms were fit with a skewed Gaussian function (log-normal fit), and fitting parameters were compared for the different experiments. The fitting parameters calculated in all three cases differed from one another by less than one increment of standard error, indicating there was no significant difference between the measured intensities. This is the expected result for a system in which CG-2 can be found in either a quenched (and therefore undetectable) or emissive state only.

Although the relative intensity of individual CG-2 molecules did not change with $[Ca^{2+}]$, the number of fluorescent molecules that could be observed did. This effect was studied in a semiquantitative way by counting the average number of molecules per image that could be detected in a series of 10 μm × 10 μm images. Quantifying this effect in a rigorous way was problematic because at low $[Ca^{2+}]$ (0−1.35 μM), a high concentration of CG-2 ($\sim 10^{-8}$ M) was needed to have a statistically relevant number of fluorescent molecules per frame, whereas at higher $[Ca^{2+}]_{free}$, CG-2 concentrations of 10^{-8} M gave rise to such a large number of molecules on the surface that reliable counting became problematic. To account for this, we adjusted the concentration of CG-2 such that a reasonable number of molecules (typically around 10) could be counted per frame and then scaled this number according to the appropriate dilution factor used for the CG-2 solution. Normalizing the number of molecules per frame against the nominal "zero" $[Ca^{2+}]_{free}$, we counted for $[Ca^{2+}]_{free}$ of 0 μM, 10 μM and above saturation (>39 μM) an average, normalized numbers of molecules per frame as around 1, 12 and 15. The corresponding normalized fluorescence intensity from the ensemble measurements give us values around 1, 18 and 36. Though the values measured in the molecule counting experiment are only semiquantitative at best, the general trend of increasing number of molecules as a function of $[Ca^{2+}]_{free}$ was clearly observed and can reasonably be correlated with the ensemble change in fluorescence intensity.

An issue that is worth addressing at this point is the effect, if any, of spin-casting on the binding between CG-2 and Ca^{2+}. One might expect that removal of water by spin-casting could influence the binding of the metal ion. It is clear from the measurements, however, that the samples remain strongly fluorescent and therefore loss of water does not drastically alter binding. It is conceivable that the differences between bulk measurements and the number of detectable molecules described above might, in part, be caused by changes in binding ability with water loss. However, we are confident that any changes caused by spin-casting are minimal.

Both the single peak in the intensity histograms and the fact that the majority of molecules exhibit single-step photobleaching indicates that the two constituent fluorophores in CG-2 are coupled rather than independent emitters. As noted in the Introduction, collective photobleaching of this kind has been observed in a wide range of multifluorophoric systems. Because of instrumental limitations, we were not able to carry out as extensive photophysical characterization for CG-2 as has been carried out for other coupled systems.[17,22,23] However, we can suggest a plausible model for explaining the behavior observed in this system. Because the single-molecule experiments were

carried out below the optical saturation threshold, we only considered models that involve excitation of a single fluorophore at a time.

We have evaluated the possibility of dipole−dipole Förster transfer taking place between the two constituent fluorophores of CG-2. Coupling of this kind can reasonably be expected in systems where the constituent fluorophore shows a relatively small Stokes shift.[33] For the CG-2 system, we have calculated the rate of energy transfer between the two constituent fluorophores using the standard expression:

$$k_{ET}(r) = \frac{Q_D \kappa^2}{\tau_f r^6}\left(\frac{9000(\ln 10)}{128\pi^5 N n^4}\right)\int_0^\infty F_D(\lambda)\,\epsilon_A(\lambda)\,\lambda^4\,d\lambda \quad (6)$$

Using the previously calculated values for the overlap integral, the experimentally measured quantum yield (∼0.73 for saturating Ca^{2+} concentrations), lifetime and estimating the geometric variables r and κ from the optimized structures in part A, we calculate a k_{ET} of around 2.4×10^{12} s^{-1}. The rate of energy transfer in this system is more than 3 orders of magnitude greater than the rate of fluorescence emission, indicating that emission can take place from either fluorophore, regardless of which fluorophore was initially excited.

On this basis, we postulate that the mechanism of coupling and hence collective photobleaching is Förster energy transfer. If one of the two fluorophores is damaged via a photochemical reaction, then the damaged fluorophore can act as a nonradiative trap site for the other. That is, if one of the constituent fluorophores bleaches, the excitation energy from the intact fluorophore can be transferred to the damaged site and lost via a nonradiative pathway. This mechanism is consistent with proposed photobleaching mechanisms in a variety of other coupled systems. For example, in their study of the fluorescent protein *Ds*Red, Lounis et al. suggested a similar mechanism to explain collective photobleaching effects and offered in partial support of this an observation of two distinct time scales in an ensemble photobleaching experiment;[17] the first time scale was associated with photobleaching of an intact protein, the second a photobleaching rate for an absorbing but not emitting (damaged) fluorophore. We have carried out similar ensemble measurements and also observed two different photobleaching time scales (data not shown), which lends support to this possible model of CG-2 bleaching.

As noted previously, a small fraction (∼6%) of molecules did show more complex photobleaching dynamics involving multiple transitions between bright and dark states ("blinking"). The emission time traces in Figure 7B-ii,iii show some of the types of photophysical behavior we observed in this small subpopulation of molecules. In trace ii, for example, one observes two discrete bursts of fluorescence, each of comparable intensity, separated by a dark state. This is the expected emission trajectory for two uncoupled fluorophores, suggesting that in some rare cases, CG-2 can adopt a conformation such that energy transfer between fluorophores is unfavorable. On other occasions, we observed traces such as Figure 7B-iii, in which there was a bright state, followed by a very brief drop in signal to the background level of the measurement, followed by a jump back to a more intense bright state. Although the emission intensity levels of the two bright states are different from one another, this trajectory is in effect quite similar to that shown in Figure 7B-ii; there are two bright states, separated by a dark (albeit short-lived) state, which again might be attributed to two uncoupled fluorophores. Differences in fluorescence intensities between the bright states may be caused by different orientations of the constituent fluorophores with respect to the polarization axis of the excitation beam. The idea that there may be several possible conformations of CG-2 is consistent with results by Hernando et al.[23] in their investigation of coupled TRITC dimers, who suggested this as a possible source of variation in emission polarization between different molecules. We anticipate that the CG-2 system should have much less conformational flexibility than the TRITC dimer system, because the binding of Ca^{2+} should constrain the system into a more rigid structure. If blinking can be attributed to rare geometrical conformations of CG-2, then it is hardly surprising that this behavior is only rarely observed.

Although the blinking dynamics of this small subpopulation of molecules is intriguing, at present, we are unable to definitively identify a mechanism for the behavior. In general, a more in-depth study of the single-molecule photophysics of this system is called for, with particular emphasis being placed on studies involving a range of higher excitation intensities to probe the possibility of higher-order bleaching processes and absorption from the excited state, as well as polarization modulation experiments and single-molecule fluorescence lifetime measurements. Efforts to expand our instrumental capabilities and explore the single-molecule photophysics of this important system are ongoing.

In summary, this paper describes the spectroscopic characterization of the calcium-sensor dye CG-2 at both the ensemble and single-molecule level. In the absence of Ca^{2+}, the dye adopts a conformation in which fluorescence is quenched by intramolecular exciton formation. Binding of Ca^{2+} gives rise to a structural change, disrupting exciton formation and results in the formation of a strongly emissive dye. Through a combination of ensemble and single-molecule spectroscopy, it was found that the bulk increase in fluorescence emission with Ca^{2+} can be attributed to a statistical increase in the number of emissive CG-2 molecules. It was found that, at the single-molecule level, CG-2 tended to photobleach in a single step, though a small subpopulation of molecules was found that bleached in two steps. Several possible photophysical models were discussed to rationalize the observed behavior, and though CG-2 appears to be well-suited for further study of fluorophore coupling in single-molecules, further investigation is need to fully understand some of the aspects of its photophysics.

Acknowledgment. This research has been supported by the Natural Sciences and Engineering Research Council of Canada (NSERC) and by the University of Saskatchewan. The Saskatchewan Structural Sciences Centre and Professor Ron Steer are acknowledged for providing access to the TCSPC system, and Dr Sophie Brunet is thanked for providing excellent technical support and advice for the fluorescence lifetime measurements. We also thank Professors Ron Steer and Stephen Urquhart for useful discussions.

References and Notes

(1) Thomas, A. P. *Nature Cell Biol.* **2000**, *2*, E126.
(2) Berridge, M. J.; Lipp, P.; Bootman, M. D. *Nature Rev. Mol. Cell Biol.* **2000**, *1*, 11.
(3) Dominguez, D. C. *Mol. Microbiol.* **2004**, *54*, 291.
(4) Falcke, M. *Adv. Phys.* **2004**, *53*, 255.
(5) Grynkiewicz, G.; Poenie, M.; Tsien, R. Y. *J. Biol. Chem.* **1985**, *260*, 3440.
(6) Tsien, R. Y. *Biochemistry* **1980**, *19*, 2396.
(7) Tsien, R.; Pozzan, T. *Methods Enzymol.* **1989**, *172*, 230.
(8) Kao, J. P. Y. Practical Aspects of Measuring Ca_2^+ with Fluorescent Indicators. In *Methods in Cell Biology*, 1994; Vol. 40, p 155.
(9) Palmer, A. E.; Jin, C.; Reed, J. C.; Tsien, R. Y. *Proc. Natl. Acad. Sci.. U.S.A.* **2004**, *101*, 17404.

(10) Truong, K.; Sawano, A.; Mizuno, H.; Hama, H.; Tong, K. I.; Mal, T. K.; Miyawaki, A.; Ikura, M. *Nature Struct. Biol.* **2001**, *8*, 1069.

(11) Miyawaki, A.; Griesbeck, O.; Heim, R.; Tsien, R. Y. *Proc. Natl. Acad. Sci.. U.S.A.* **1999**, *96*, 2135.

(12) Brasselet, S.; Peterman, E. J. G.; Miyawaki, A.; Moerner, W. E. *J. Phys. Chem. B* **2000**, *104*, 3676.

(13) Minta, A.; Kao, J. P. Y.; Tsien, R. Y. *J. Biol. Chem.* **1989**, *264*, 8171.

(14) Haugland, R. P. *Handbook of fluorescent probes and research products*, 9th ed.; Molecular Probes Inc.: 2002.

(15) Kasha, M.; Rawls, H. R.; Ashraf El-Bayoumi, M. *Int. Union Pure Appl. Chem.* **1965**, *11*, 371.

(16) Bopp, M. A.; Jia, Y. W.; Li, L. Q.; Cogdell, R. J.; Hochstrasser, R. M. *Proc. Natl. Acad. Sci.. U.S.A.* **1997**, *94*, 10630.

(17) Lounis, B.; Deich, J.; Rosell, F. I.; Boxer, S. G.; Moerner, W. E. *J. Phys. Chem. B* **2001**, *105*, 5048.

(18) Ha, T.; Enderle, T.; Ogletree, D. F.; Chemla, D. S.; Selvin, P. R.; Weiss, S. *Proc. Natl. Acad. Sci.. U.S.A.* **1996**, *93*, 6264.

(19) van Oijen, A. M.; Ketelaars, M.; Kohler, J.; Aartsma, T. J.; Schmidt, J. *Science* **1999**, *285*, 400.

(20) VandenBout, D. A.; Yip, W. T.; Hu, D. H.; Fu, D. K.; Swager, T. M.; Barbara, P. F. *Science* **1997**, *277*, 1074.

(21) Yip, W. T.; Hu, D. H.; Yu, J.; Vanden Bout, D. A.; Barbara, P. F. *J. Phys. Chem. A* **1998**, *102*, 7564.

(22) Ying, L. M.; Xie, X. S. *J. Phys. Chem. B* **1998**, *102*, 10399.

(23) Hernando, J.; van der Schaaf, M.; van Dijk, E.; Sauer, M.; Garcia-Parajo, M. F.; van Hulst, N. F. *J. Phys. Chem. A* **2003**, *107*, 43.

(24) Chibisov, A. K.; Zakharova, G. V.; Gorner, H. *Phys. Chem. Chem. Phys.* **2001**, *3*, 44.

(25) Chen, R. F.; Knutson, J. R. *Anal. Biochem.* **1988**, *27*, 61.

(26) Weinstein, J. N.; Yoshikami, S.; Henkart, P.; Blumenthal, R.; Hagins, W. A. *Science* **1977**, *195*, 489.

(27) Schauer, C. K.; Anderson, O. P. *J. Am. Chem. Soc.* **1987**, *109*, 3646.

(28) Barnett, B. L.; Uchtman, V. A. *Inorg. Chem.* **1979**, *18*, 2674.

(29) Du, H.; Fuh, R. C. A.; Li, J. Z.; Corkan, L. A.; Lindsey, J. S. *Photochem. Photobiol.* **1998**, *68*, 141.

(30) Sanders, R.; Gerritsen, H. C.; Draaijer, A.; Houpt, P. M.; Levine, Y. K. *Bioimaging* **1994**, *2*, 131.

(31) Bagh, S.; Paige, M. F. *Can. J. Chem.—Rev. Can. Chim.* **2005**, *83*, 435.

(32) Schmidt, T.; Schutz, G. J.; Baumgartner, W.; Gruber, H. J.; Schindler, H. *J. Phys. Chem.* **1995**, *99*, 17662.

(33) Lakowicz, J. *Principles of fluorescence spectrosopy*, 2nd ed.; Kluwer Academic: New York, 1999.